Cancer Chemother Pharmacol (2012) 69:85–90
DOI 10.1007/s00280-011-1675-z

ORIGINAL ARTICLE

Modification of uptake and subcellular distribution of doxorubicin by *N*-acylhydrazone residues as visualised by intrinsic fluorescence

Katharina Effenberger-Neidnicht · Sandra Breyer · Katharina Mahal · Florenz Sasse · Rainer Schobert

Received: 15 January 2011 / Accepted: 7 May 2011 / Published online: 24 May 2011

Abstract
Purpose Doxorubicin (**1**) is commonly used in the treatment of a wide range of cancers. Some *N*-acylhydrazones of **1** were previously found to have an improved tumour and organ selectivity. In order to clarify the molecular basis for this effect, the cellular uptake into various cancer cells and the localisation in PtK_2 potoroo kidney cells of **1** and its *N*-acylhydrazones derived from heptadecanoic acid (**2**) and 11-(menthoxycarbonyl)undecanoic acid (**3**) were studied drawing on their intrinsic fluorescence.
Methods The uptake of compounds **1–3** into human cells of HL-60 leukaemia, 518A2 melanoma, HT-29 colon, and resistant KB-V1/Vbl and MCF-7/Topo breast carcinomas was determined fluorometrically from their residual amounts in the supernatant. Their time-dependent accumulation in PtK_2 potoroo kidney cells was visualised by fluorescence microscopy.
Results The uptake, though not the cytotoxicity, of **2** in multi-drug resistant MCF-7/Topo breast cancer cells was conspicuously greater than that of **1** and **3**, probably due to an attractive lipophilic interaction with the lipid-rich membranes of these cells. In non-malignant PtK_2 cells, both **1** and **3** accumulated initially in the nuclei. Upon prolonged incubation, their fluorescent metabolites were visualised in lysosomes neighbouring the nuclei. In contrast, conjugate **2** was not observed in the nuclei at any time. After 2 h, it had accumulated in vesicles scattered all over the cells, and upon prolonged incubation, its fluorescent metabolites were concentrated in the cellular membrane.
Conclusions Long unbranched fatty acyl residues when attached to doxorubicin via a hydrazone can act as lipophilic membrane anchors. This allows an increased uptake of such derivatives into lipid-rich membranes especially of multi-drug resistant cancer cells, a retarded release from there into the cytosol and the eventual storage of their metabolites again in the cell membrane rather than in lysosomes.

Keywords Doxorubicin · Fluorescence spectroscopy · PtK_2 cells · Conjugates · Membrane lipids · Fatty acids

K. Effenberger-Neidnicht · S. Breyer · K. Mahal · R. Schobert (✉)
Organic Chemistry Laboratory, University Bayreuth, Universitaetsstrasse 30, NW 1, 95447 Bayreuth, Germany
e-mail: Rainer.Schobert@uni-bayreuth.de

F. Sasse
Department of Chemical Biology, Helmholtz Centre for Infection Research (HZI), Inhoffenstrasse 7, 38124 Braunschweig, Germany

Introduction

Doxorubicin (**1**), a *Streptomyces* metabolite, is used in chemotherapy against a wide range of cancers such as haematological malignancies, soft tissue sarcomas, lymphomas and various types of carcinomas despite its clinical limitations such as cardiotoxicity and induction of multi-drug resistance [1–6]. In earlier studies, we had shown that some *N*-acylhydrazones of **1** derived from long-chain fatty acids or terpenes have a higher tumour and organ selectivity than **1** while sharing with it the same mechanism of apoptosis induction, characterised by elevated levels of reactive oxygen species and apoptosis-relevant caspases and a loss of the mitochondrial membrane potential. Some of these new hydrazone conjugates not only had a greater selectivity than the parent drug **1** [7, 8] but were also less good substrates for the ABC transporters of multi-drug resistant cancer cells. In order to clarify the molecular basis

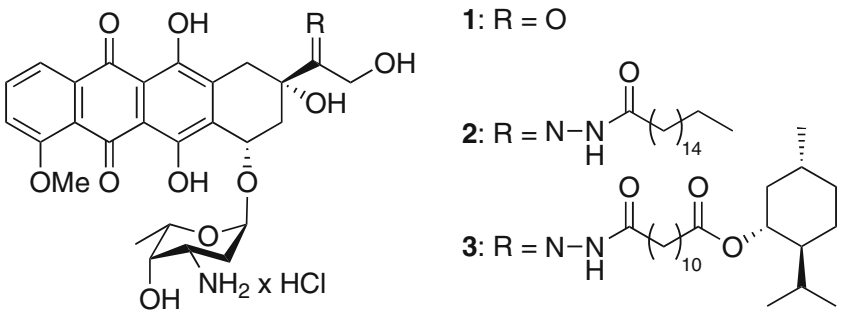

Fig. 1 Structures of doxorubicin (**1**) and its *N*-heptadecanoylhydrazone **2** and 11-(menthoxycarbonyl)undecanoylhydrazone **3**

for these effects, we now studied the cellular uptake of **1** and its *N*-acylhydrazones derived from heptadecanoic acid (**2**) and 11-(menthoxycarbonyl)undecanoic acid (**3**) by various cancer cells and their localisation in flat, easy to visualise PtK_2 potoroo (*Potorous tridactylis*) kidney epithelial cells by means of their intrinsic fluorescence (Fig. 1).

Materials and methods

General

The hydrazones **2** and **3** were prepared as described previously [7]. Fluorescence spectra were recorded on an FP-6500 fluorescence spectrophotometer (JASCO, Tokyo, Japan) between 500 and 700 nm. Uptake of the derivatives was measured using a CM Infinite F200 fluorescence plate reader with excitation and emission wavelengths of 485/20 and 590/20 nm (TECAN, Crailsheim, Germany), respectively. Fluorescence analyses of treated cells were conducted with an Axioplan fluorescence microscope equipped with an Axiocam camera (ZEISS, Jena, Germany) and evaluated with the software AxioVision 3.1.

Cell lines and culture conditions

Leukaemia HL-60 cells were obtained from the German Collection of Biological Material (DSMZ), Braunschweig (Germany), melanoma 518A2 cells from the Department of Oncology and Hematology of the Martin Luther University, Halle-Wittenberg (Germany), KB-V1/Vbl cervix and MCF-7/Topo breast carcinoma cells from the Institute of Pharmacy of the University Regensburg (Germany) and HT-29 colon carcinoma cells as well as human foreskin fibroblasts (HF) from the University Hospital Erlangen (Germany). The HL-60 and HT-29 cells were grown in RPMI-1640 medium supplemented with 10% foetal calf serum (FCS), 100 IU mL^{-1} penicillin G, 100 μg mL^{-1} streptomycin sulphate, 0.25 μg mL^{-1} amphotericin B and 250 μg mL^{-1} gentamycin (all GIBCO). The 518A2, the HF and the KB-V1/Vbl cells were cultured in Dulbecco's modified Eagle medium (DMEM, GIBCO), containing 10% FCS, 100 IU mL^{-1} penicillin G, 100 μg mL^{-1} streptomycin sulphate, 0,25 μg mL^{-1} amphotericin B and 250 μg mL^{-1} gentamycin. The MCF-7/Topo cells were grown in Eagle's minimal essential medium with Earle's salts (MEM; SIGMA) supplemented with 2.2 g L^{-1} $NaHCO_3$, 110 mg L^{-1} sodium pyruvate and 5% FCS. The potoroo kidney cells PtK_2 were obtained from the American Type Culture Collection (ATCC) and cultivated in MEM (GIBCO) supplemented with 10% FCS and non-essential amino acids (GIBCO). They were maintained in a moisture-saturated atmosphere (5% CO_2) at 37°C in 50-mL culture flasks (NUNC, Germany) and serially passaged after trypsinisation.

Fluorescence spectroscopy

A JASCO FP-6500 fluorescence spectrophotometer was used for fluorescence measurements of compounds **1–3** dissolved in phosphate-buffered saline (5 μM). The excitation wavelength was 490 nm, and emission wavelengths ranged from 500 to 650 nm.

Cellular drug uptake

The cellular uptake of the test compounds was ascertained using a TECAN CM Infinite F200 fluorescence plate reader (Exc.: 485/25 nm, Em.: 590/20 nm). Typically, 500 μL cells of HL-60 leukaemia (5×10^5 mL^{-1}), HT-29 colon carcinoma, 518A2 melanoma, KB-V1/Vbl cervix carcinoma and MCF-7/Topo breast carcinoma (each 5×10^4 mL^{-1}) were incubated in 24-well plates with the compounds **1**, **2** or **3** (5 μM) for 3 h. The medium was removed by centrifugation for 5 min at 150*g*. The residual fluorescence intensity was measured in the supernatant, and the corresponding concentration of test compounds taken up by the cells was calculated by comparison with identically treated references [9].

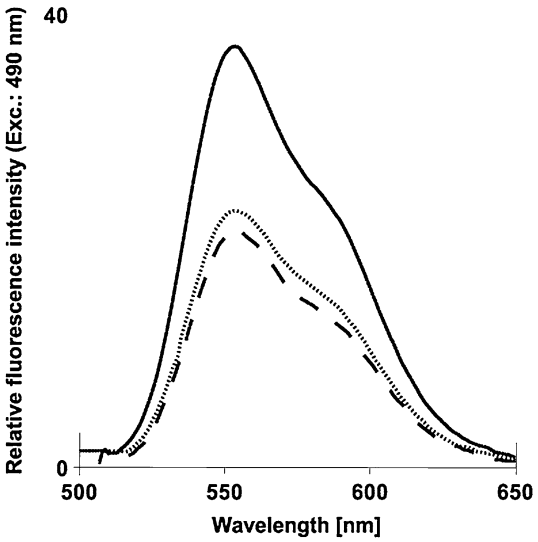

Fig. 2 Fluorescence spectra of doxorubicin (**1**) (*solid line*) and its *N*-acyl hydrazones **2** (*dotted line*) and **3** (*broken line*) following excitation at 490 nm

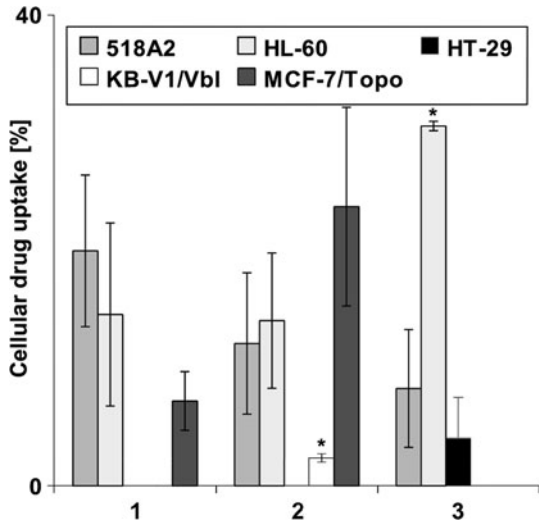

Fig. 3 Uptake of doxorubicin (**1**) and its *N*-acyl hydrazones **2** and **3** into cells of 518A2 melanoma, HL-60 leukaemia, HT-29 colon carcinoma, KB-V1/Vbl cervix carcinoma and MCF-7/Topo breast carcinoma upon incubation with 5 μM concentrations for 3 h. Column heights represent means of three independent experiments, *bars* indicate SD. **P* values of <0.05 versus control were considered to be significant

Statistical analysis of measurement results

The results are expressed as means ± standard deviation (SD). The Student–Newman–Keuls test was used to determine statistical significance with P value < 0.05 considered significant (*).

Cellular localisation

The distribution of the test compounds in PtK_2 cells was visualised via fluorescence microscopy. Typically, the cells were grown in DMEM (750 μL) in 4-well plates (Nunc) on glass coverslips and incubated with the test compounds **1**, **2** or **3** (10 μM) for periods ranging from 2 to 16 h. The medium was removed, the cells were washed twice with phosphate-buffered saline (PBS) and mounted vital in PBS. The Hoechst dye 33342 was optionally added (5 μg mL^{-1}) to stain the nuclei, and the cells were imaged using a ZEISS Axioplan fluorescence microscope [9, 10].

Results

Fluorescence spectroscopy

Fluorescence spectroscopy has been frequently employed to study the interaction of doxorubicin (**1**), e.g., with DNA in the course of intercalation [11, 12] or with lipid membranes [13]. We now measured the fluorescence spectra of the test compounds **1**–**3** in phosphate-buffered saline (PBS; 5 μM) at pH 7.4. Since the fluorophore of **1** has a known absorption maximum between 480 and 500 nm [14], we excited the test compounds at 490 nm and observed three congruent fluorescence spectra (Fig. 2). They are each characterised by an overlay of three bands resulting in an envelope curve with a maximum around 550 nm and a shoulder at ca. 580 nm. However, the intensities of the spectra of the hydrazone conjugates **2** and **3** were only about half of that of **1** itself. This is qualitatively in keeping with a report by Chourpa et al. [15] on the changes of the intrinsic fluorescence of **1** upon addition of sodium oleate. The authors explained this pH- and ratio-dependent effect by lipophilic interactions of the aromatic fluorophore of **1** with the long alkenyl chain of oleic acid. A similar and obviously more intense lipophilic interaction could result from a backfolding of the covalently attached heptadecanoyl chain of **2** or of the tethered menthyl residue of **3**, respectively, on top of the anthraquinone fluorophore.

Cellular drug uptake

Next, we ascertained the uptake of **1** and its derivatives **2** and **3** by five human cancer cell lines of entities that are typically treated with **1**, namely leukaemia, melanoma as well as breast, cervix and colon carcinomas. The cells were incubated with 5 μM of **1**–**3** for 3 h, and the residual fluorescence intensity in the supernatant following incubation was measured after a centrifugation step. The per cent cellular drug uptake relative to reference solutions was calculated and plotted as shown in Fig. 3 [9]. All test

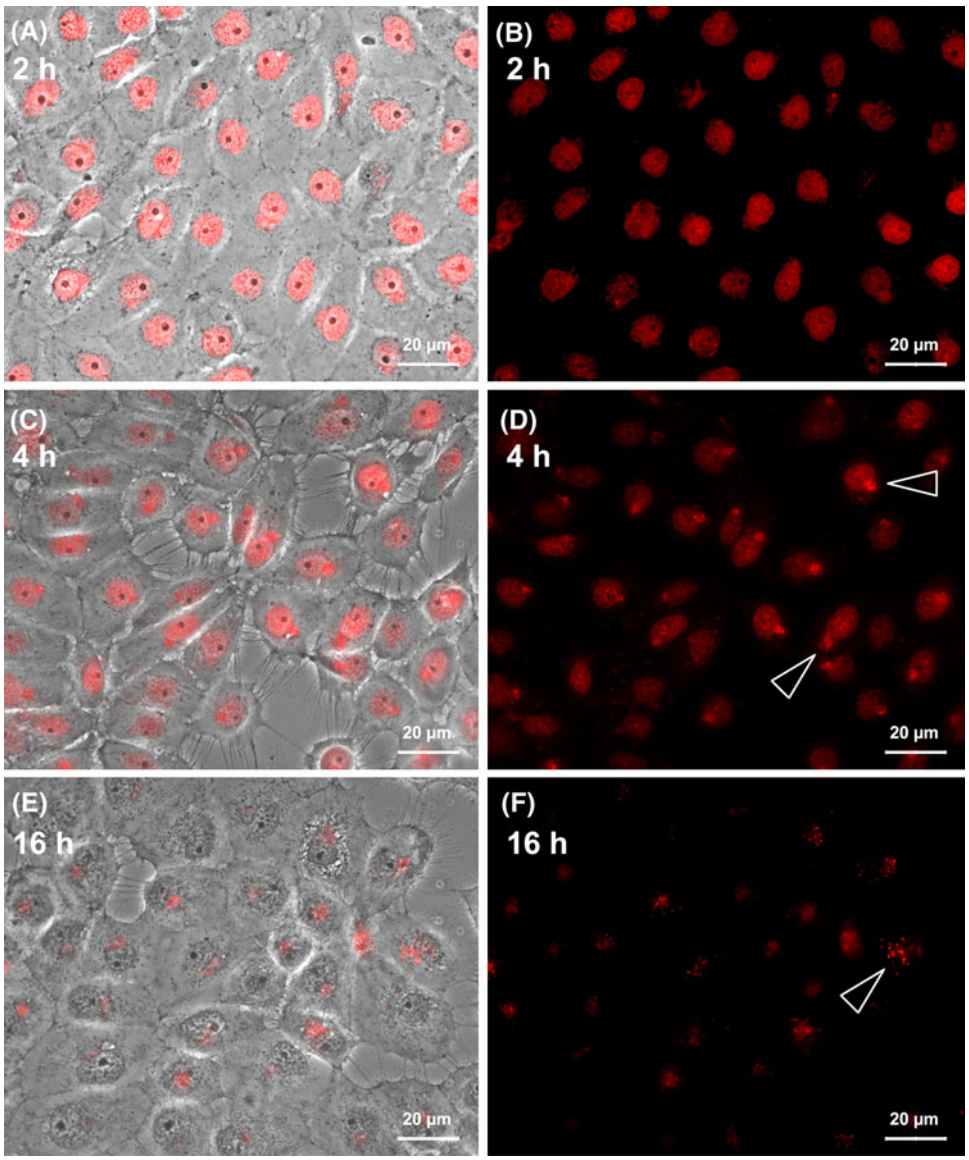

Fig. 4 PtK_2 cells were incubated with **1** (10 µM) for 2 h (**a**, **b**), or 4 h (**c**, **d**) or 16 h (**e**, **f**), then mounted vital in PBS and imaged by fluorescence microscopy. The accumulation of **1** in cytoplasmic vesicles is marked by *arrowheads*. *Left column* overlay of brightfield and fluorescence channels; *right column* fluorescence channel only

compounds accumulated strongly in the 518A2 and the HL-60 cells which corresponds well with their previously reported high cytotoxicity against these cell lines [7]. In contrast, their accumulation in the remaining three multi-drug resistant cancer cell lines was comparatively low, which in fact matches their low cytotoxicity in these cells. However, fatty acid conjugate **2** is an exception since it was selectively and significantly (>20%) accumulated in multi-drug resistant MCF-7/Topo breast carcinoma cells.

Cellular localisation

Finally, to analyse the cellular localisation of **1** and its derivatives **2** and **3**, non-malignant PtK_2 potoroo kidney cells were incubated with 10 µM concentrations of them for up to 16 h, then mounted vital in PBS and imaged using fluorescence microscopy. The results of these autofluorescence analyses are shown in Figs. 4 and 5.

While after 2 h of incubation, **1** was localised only in PtK_2 nuclei (Fig. 4a, b), upon prolonged exposure, it or its fluorescent metabolites were accumulated in vesicles which were initially neighbouring the nuclei (Fig. 4c, d) but later were distributed throughout the cells (Fig. 4e, f). This is in line with the previously reported uptake and subcellular distribution of **1** in other cells, e.g., rat embryo fibroblasts and human myeloid leukaemia cells [9, 10]. For the menthyl-terminated hydrazone **3**, we found a subcellular localisation similar to that of **1**, albeit proceeding more slowly. The accumulation in the nuclei required twice as long (4 h) for completion as in the case of the parent drug. However, again some differences emerged for conjugate **2**. Here, no drug was found in PtK_2 nuclei at any

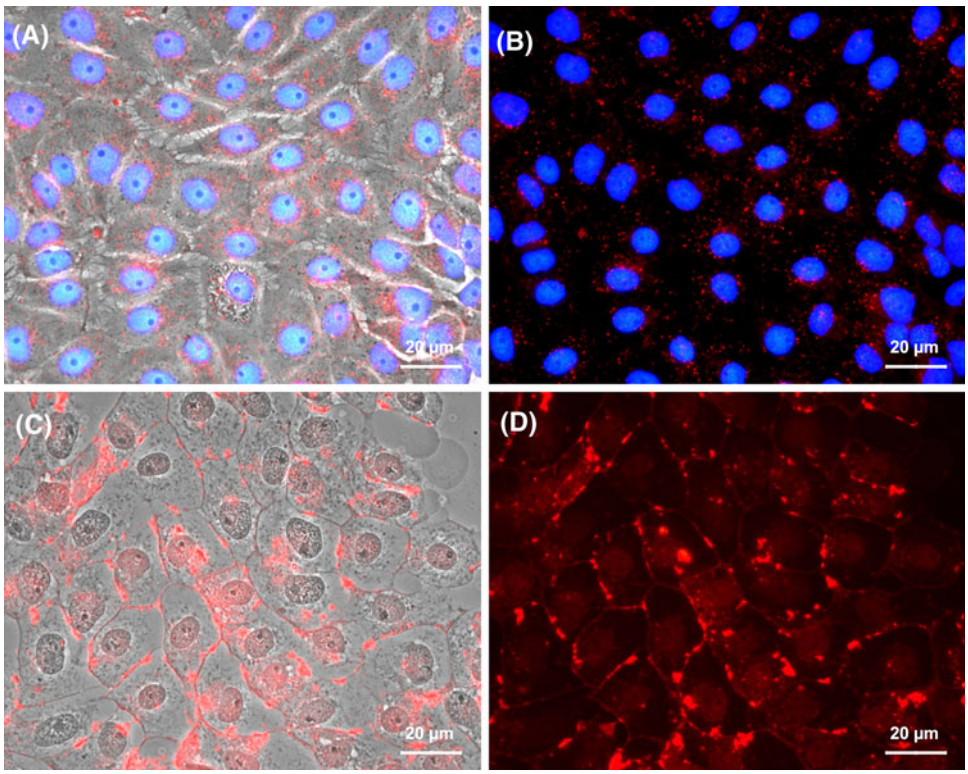

Fig. 5 PtK_2 cells were incubated with **2** (10 µM) for 2 h (**a**, **b**) or 16 h (**c**, **d**), then mounted vital in PBS and imaged by fluorescence microscopy. Cell nuclei in panels *A* and *B* were additionally stained with Hoechst dye 33342. *Left column* brightfield plus fluorescence channels; *right column* fluorescence channel only

time but in vesicles throughout the cell yet after incubation periods as short as 2 h (Fig. 5a, b). This was confirmed by co-localisation experiments with the nuclei-staining Hoechst dye 33342. Upon prolonged incubation, **2** or its fluorescent metabolites penetrated into the cellular membrane giving rise to intensive fluorescence there (Fig. 5c, d). We assume that the long linear fatty acyl residue acts as a lipophilic anchor, thus immobilising the conjugate or a metabolite of it at the membrane. This would not be possible for **1** or **2** which lack such a straight lipophilic tether.

Discussion

The cell membrane of resistant cancer cells is rich in lipids with saturated hydrophobic acyl chains, neutral and sphingomyelin lipids, which can attractively interact with doxorubicin [16]. Very recently, Labhasetwar et al. [17] reported that doxorubicin penetrates into the highly organised lipid monolayers of resistant MCF-7 breast cancer cell membranes and is retained there. This strong lipid-drug interaction is also believed to reduce the ability of the drug to diffuse across the cell membrane and into the cytosol, and to enhance the likelihood of near-by ABC efflux transporters expelling the drug [18]. The fatty acyl conjugate **2** can intertwine even more effectively than **1** with the membrane lipids of resistant MCF-7 cells. This would explain its enhanced uptake into these cells which, however, does not lead to an increased cytotoxicity. The IC_{50}(24 h) values of **1** and **2** against MCF-7/Topo cells are virtually identical (ca 6 µM) [7]. In contrast, the cell membranes of sensitive cancer cells and of non-malignant cells feature a lower lipid packing density and so allow drugs to diffuse across the bilayer without much lipophilic retardation. The most import interactions of doxorubicin with such cell membranes are thought to be electrostatic ones between its amino sugar moiety and negatively charged phospholipids [17, 19]. This is in keeping with the relatively high uptake of all test compounds **1**–**3** by sensitive 518A2 melanoma and HL-60 leukaemia cells as well as by the non-tumour derived PtK_2 potoroo kidney cells. **1** and its terpenyl conjugate **3** were initially accumulated in the PtK_2 nuclei and eventually degraded to fluorescent metabolites disposed of in cytoplasmic vesicles, e.g. lysosomes. In contrast, the fatty acyl conjugate **2** or its metabolites, respectively, were not observed in the nuclei at any time, but were rather localised in secretory vesicles after 2 h and attached to the plasma membrane after 16 h. We assume that while all compounds **1**–**3** are degraded in the cells to the respective aglycon, only that originating from **2** possesses a linear lipid anchor suitable for a persistent attachment to the plasma membrane. It remains contentious whether interference of doxorubicin and its derivatives with the nuclear or nucleolar structure of PtK_2 cells is correlated with their cytotoxicity [20].

Acknowledgments We thank the Deutsche Forschungsgemeinschaft for financial support (grant Scho 402/8-3) and Ribosepharm GmbH (Germany) for a free batch of doxorubicin.

Conflicts of interest None.

References

1. Robert J (1998) Anthracyclines. In: Grochow LB, Ames MM (eds) A clinician′s guide to chemotherapy, pharmcokinetics and pharmacodynamics. Williams and Wilkins, Baltimore, pp 93–173
2. Cragg GM, Grothaus PG, Newman DJ (2009) Impact of natural products on developing new anti-cancer agents. Chem Rev 109:3012–3043
3. Colucci MA, Moody CJ, Couch GD (2008) Natural and synthetic quinones and their reduction by the quinone reductase enzyme NQO1: from synthetic organic chemistry to compounds with anticancer potential. Org Biomol Chem 6:637–656
4. Bolton JL, Trush MA, Penning TM, Dryhurst G, Monks TJ (2000) Role of quinones in toxicology. Chem Res Toxicol 13:135–160
5. Minotti G, Menna P, Salvatorelli E, Cairo G, Gianni L (2004) Anthracyclines: molecular advances and pharmacologic developments in antitumor activity and cardiotoxicity. Pharmacol Rev 56:185–229
6. Gewirtz DA (1999) A critical evaluation of the mechanisms of action proposed for the antitumor effects of the anthracycline antibiotics adriamycin and daunorubicin. Biochem Pharmacol 57:727–741
7. Effenberger K, Breyer S, Schobert R (2010) Modulation of doxorubicin activity in cancer cells by conjugation with fatty acyl and terpenyl hydrazones. Eur J Med Chem 45:1947–1954
8. Effenberger K, Breyer S, Ocker M, Schobert R (2010) New doxorubicin N-acyl hydrazones with improved efficacy and cell line specificity show modes of action different from the parent drug. Int J Clin Pharmacol Ther 48:485–486
9. Noël G, Peterson C, Trouet A, Tulkens R (1978) Uptake and subcellular localization of daunorubicin and adriamycin in cultured fibroblasts. Eur J Cancer 14:363–368
10. Hurwitz SJ, Terashima M, Mizunuma N, Slapka CA (1997) Vesicular anthracycline accumulation in doxorubicin-selected U-937 cells: participation of lysosomes. Blood 89:3745–3754
11. Pietrzak M, Wieczorek Z, Stachelska A, Darzynkiewicz Z (2003) Interactions of chlorophyllin with acridine orange, quinacrine mustard and doxorubicin analyzed by light absorption and fluorescence spectroscopy. Biophys Chem 104:305–313
12. Szulawska A, Gniazdowski M, Czyz M (2005) Sequence specificity of formaldehyde-mediated covalent binding of anthracycline derivatives to DNA. Biochem Pharmacol 69:7–18
13. Karukstis KK, Thompson EHZ, Whiles JA, Rosenfeld RJ (1998) Deciphering the fluorescence signature of daunomycin and doxorubicin. Biophys Chem 73:249–263
14. Du H, Fuh RA, Li J, Corkan A, Lindsey JS (1998) PhotochemCAD: A computer-aided design and research tool in photochemistry. Photochem Photobiol 68:141–142
15. Munnier E, Tewes F, Cohen-Jonathan S, Linassier C, Douziech-Eyrolles L, Marchais H, Soucé M, Hervé K, Dubois P, Chourpa I (2007) On the interaction of doxorubicin with oleate ions: fluorescence spectroscopy and liquid-liquid extraction study. Chem Pharm Bull 55:1006–1010
16. Ramu A, Glaubiger D, Magrath IT, Joshi A (1983) Plasma membrane lipid structural order in doxorubicin-sensitive and resistant P388 cells. Cancer Res 43:5533–5537
17. Peetla C, Bhave R, Vijayaraghavalu S, Stine A, Kooijman E, Labhasetwar V (2010) Drug resistance in breast cancer cells: biophysical characterization of and doxorubicin interactions with membrane lipids. Mol Pharm 7(6):2334–2348
18. Lu P, Liu R, Sharom FJ (2001) Drug transport by reconstituted P-glycoprotein in proteoliposomes. Effect of substrates and modulators, and dependence on bilayer phase state. Eur J Biochem 268:1687–1697
19. Goormaghtigh E, Chatelain P, Caspers J, Ruysschaert JM (1980) Evidence of a specific complex between adriamycin and negatively charged phospholipids. Biochim Biophys Acta 597:1–14
20. Jensen CG, Wilson WR, Bleumink AR (1985) Effects of amsacrine and other DNA-intercalating drugs on nuclear and nucleolar structure in cultured V79 Chinese hamster cells and PtK2 rat kangaroo cells. Cancer Res 45:717–725